



## Discovery of *N*-(1-adamantyl)-2-(4-alkylpiperazin-1-yl)acetamide derivatives as T-type calcium channel (Ca<sub>v</sub>3.2) inhibitors

Fabrizio Giordanetto<sup>a,\*</sup>, Laurent Knerr<sup>a</sup>, Nidhal Selmi<sup>a</sup>, Antonio Llinàs<sup>b</sup>, Anders Lindqvist<sup>c</sup>, Qing-Dong Wang<sup>c</sup>, Pernilla Ståhlberg<sup>a</sup>, Fredrik Thorstensson<sup>a</sup>, Victoria Ullah<sup>a</sup>, Kristina Nilsson<sup>a</sup>, Gavin O'Mahony<sup>a</sup>, Ågot Högborg<sup>c</sup>, Emma Lindhardt<sup>b</sup>, Annika Åstrand<sup>c</sup>, Göran Duker<sup>c</sup>

<sup>a</sup> Medicinal Chemistry, AstraZeneca R&D CVGI iMed, Pepparedsleden 1, SE-431 83 Mölndal, Sweden

<sup>b</sup> DMPK, AstraZeneca R&D CVGI iMed, Pepparedsleden 1, SE-431 83 Mölndal, Sweden

<sup>c</sup> Bioscience, AstraZeneca R&D CVGI iMed, Pepparedsleden 1, SE-431 83 Mölndal, Sweden

### ARTICLE INFO

#### Article history:

Received 18 May 2011

Revised 16 June 2011

Accepted 19 June 2011

Available online 30 June 2011

#### Keywords:

Calcium channel inhibition

Ca<sub>v</sub>3.2

T-type calcium channels

### ABSTRACT

Chemical evolution of a HTS-based fragment hit resulted in the identification of *N*-(1-adamantyl)-2-[4-(2-tetrahydropyran-4-ylethyl)piperazin-1-yl]acetamide, a novel, selective T-type calcium channel (Ca<sub>v</sub>3.2) inhibitor with in vivo antihypertensive effect in rats.

© 2011 Elsevier Ltd. All rights reserved.

Calcium influx across the cellular membrane is partly controlled by a family of transmembrane proteins termed voltage-gated calcium channels. These are activated by changes in electrical potential difference across the membrane and have been classified into different subtypes according to various considerations: Ca<sub>v</sub>1.x (L-type), Ca<sub>v</sub>2.x (N-, P/Q- and R-type), and Ca<sub>v</sub>3.x (T-type).<sup>1</sup>

The T-type class is characterized by fast inactivation (transient) and small conductance (tiny), and is composed of three members based on the different main pore-forming  $\alpha$ 1 subunit: Ca<sub>v</sub>3.1 ( $\alpha$ 1G), Ca<sub>v</sub>3.2 ( $\alpha$ 1H) and Ca<sub>v</sub>3.3 ( $\alpha$ 1I).<sup>1</sup> While Ca<sub>v</sub>3.1 and Ca<sub>v</sub>3.3 are mainly expressed in the brain, Ca<sub>v</sub>3.2 is found in brain and peripheral tissues (e.g., heart, kidney, liver).<sup>2</sup>

In addition to their implications in a multitude of disease states, T-type channels were proposed as therapeutic targets for a number of cardiovascular afflictions including hypertension,<sup>3</sup> angina pectoris,<sup>3</sup> heart failure,<sup>4</sup> and atrial fibrillation.<sup>5,6</sup> Specifically, in the cardiovascular system, T-type calcium channels are mainly involved in cardiac pacemaking<sup>7,8</sup> and vascular smooth muscle contraction regulation.<sup>9,10</sup> Although several groups have reported T-type channels inhibitors (for a recent review see<sup>11</sup>), the cardiovascular pharmacology of T-type blockers has remained elusive due to the difficulties in characterizing the T-type current (*I*<sub>CaT</sub>) in the human heart.<sup>12</sup>

Mibefradil (Fig. 1), the archetypal T-type channel inhibitor, was launched in 1997 as an effective antihypertensive agent only to be later withdrawn from the market due to the severity of observed drug–drug interactions. As part of our efforts to discover novel treatments for atrial fibrillation (AF), we were particularly intrigued by Mibefradil's ability to protect against atrial remodeling, a key contributing factor to AF's own exacerbation, in a dog model of AF.<sup>5,6</sup> Although the ion channel selectivity of Mibefradil has been questioned in vitro and in vivo, we hypothesized that a T-type selective inhibitor could afford a similar cardioprotective effect to Mibefradil. This is corroborated by the fact that Diltiazem (an L-type calcium channel inhibitor) did not show any cardioprotective effect in the same AF dog model.<sup>6</sup> Furthermore, as Ca<sub>v</sub>3.2 is the main T-type isoform expressed in the heart, we resolved to identify Ca<sub>v</sub>3.2 inhibitors to verify our initial hypothesis.

High-throughput electrophysiology screening using a QPatchHTX instrument (Sophion Bioscience A/S, Ballerup, Denmark) and hit-triaging identified fragment **1** as a weak Ca<sub>v</sub>3.2 inhibitor (IC<sub>50</sub>: 70  $\mu$ M). Nevertheless, we considered it an attractive starting point for further chemical evolution due its favorable size and lipophilicity attributes (MW: 277; *c log P*: 1.7), and the readily availability of structure–activity relationships (SAR) from nearest fragment neighbors. We also realized the structural similarity between **1** and TTA-P1, a T-type inhibitor previously reported by Merck,<sup>13</sup> and decided to verify whether potency improvements could be afforded through series hybridization. As a result, compounds **2–4** were prepared according to Scheme 1. Progressive growth of the alkyl group

\* Corresponding author. Tel.: +46 31 7065723; fax: +46 31 7763710.

E-mail address: [fabrizio.giordanetto@astrazeneca.com](mailto:fabrizio.giordanetto@astrazeneca.com) (F. Giordanetto).

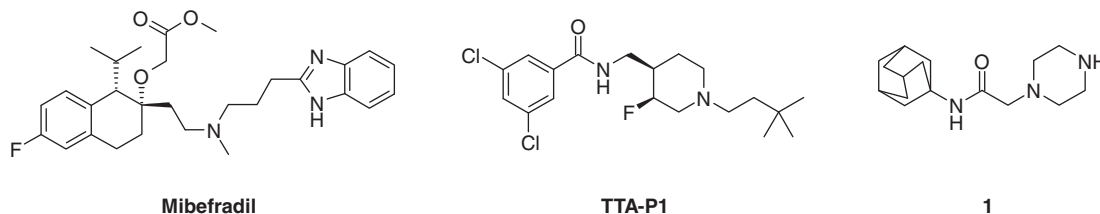
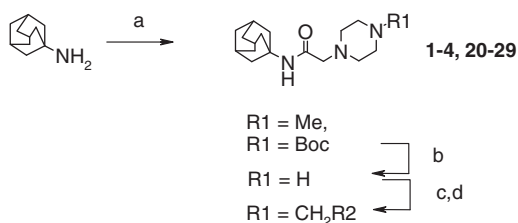


**Figure 1.** Selected T-type calcium channel inhibitors (Mibefradil, **TTA-P1**) and initial fragment hit **1**.



**Scheme 1.** General synthesis of diverse *N*-alkylated piperidines. Reagents and conditions: (a) (i) 2-chloroacetyl chloride, DIEA, DCM 0–20 °C, 16 h, 92%, (ii) *tert*-butyl piperazine-1-carboxylate or 1-methylpiperazine, K<sub>2</sub>CO<sub>3</sub>, acetonitrile, reflux, 4 h, 85–90%; (b) TFA, DCM, 20 °C, 16 h, 90%; (c) R<sub>2</sub>CHO, NaBH(OAc)<sub>3</sub>, CH<sub>3</sub>COOH, MeOH, 20 °C, 16 h or R<sub>2</sub>CH<sub>2</sub>Br/Cl, K<sub>2</sub>CO<sub>3</sub>, acetonitrile, reflux, 5 h (or 120 °C, *μ*w, 45 min) or (i) R<sub>2</sub>CH<sub>2</sub>OH, Dess–Martin periodinane, NaHCO<sub>3</sub>, DCM, 20 °C, 3 h, (ii) NaBH(OAc)<sub>3</sub>, DCM, 20 °C, 16 h, 24–81%; (d) For **29**: NaBH<sub>4</sub>, MeOH, 20 °C, 2 h, 82%.

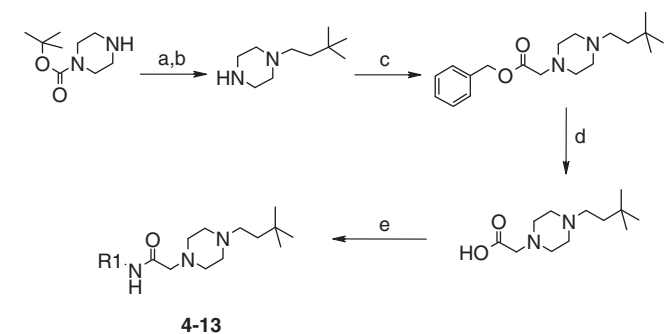
**Table 1**  
Ca<sub>v</sub>3.2 potency and ligand efficiencies for compounds **1–4**

Compound	R1	Ca <sub>v</sub> 3.2 IC <sub>50</sub> <sup>a</sup> (μM)	LE <sup>b</sup>	LipE <sup>c</sup>
<b>1</b>	H	70	0.28	2.5
<b>2</b>	Me	30	0.29	3.3
<b>3</b>		2	0.31	2.5
<b>4</b>		0.8	0.32	2.5
Mibefradil		1	0.23	–0.4
<b>TTA-P1</b>		0.2	0.37	1.1

<sup>a</sup> Results are mean of at least two experiments. Experimental errors within 20% of value.<sup>22</sup>

<sup>b</sup> Ligand efficiency (LE): calculated as –RTln(IC<sub>50</sub>)/HAC.

<sup>c</sup> Lipophilicity efficiency (LipE): calculated as pIC<sub>50</sub> – c log *P*.



**Scheme 2.** Synthesis of the 'adamantane replacement' set. Reagents and conditions: (a) 3,3-dimethylbutyraldehyde, NaBH(OAc)<sub>3</sub>, MeOH, 20 °C, 16 h; (b) TFA, DCM, 20 °C, 95% over two steps; (c) benzyl bromoacetate, K<sub>2</sub>CO<sub>3</sub>, acetone, 60 °C, 40 h, 92%; (d) H<sub>2</sub>, 10% Pd/C, EtOH, 20 °C, 2 h, 95%; (e) R<sub>1</sub>NH<sub>2</sub>, EDAC, HOBT, DCM/water (7:2), 20 °C, 16 h, 5–60%.

**Table 2**

Ca<sub>v</sub>3.2 potency and metabolic stability for compounds in the 'adamantane replacement' set

Compound	R1	Ca <sub>v</sub> 3.2 IC <sub>50</sub> <sup>a</sup> (μM)	HLM Cl <sub>int</sub> <sup>b</sup> (μL/min/mg)
<b>4</b>		0.8	48
<b>5</b>		>30	<5
<b>6</b>		2	36
<b>7</b>		14.6	<5
<b>8</b>		8.8	26
<b>9</b>		7.3	12.5
<b>10</b>		15.2	3
<b>11</b>		1.5	33
<b>12</b>		>30	<5
<b>13</b>		0.9	<5

<sup>a</sup> Results are mean of at least two experiments. Experimental errors within 20% of value.<sup>22</sup>

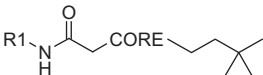
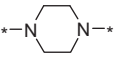
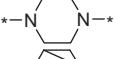
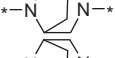
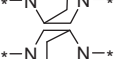
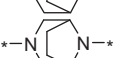
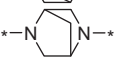
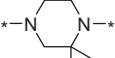
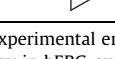
<sup>b</sup> Rate of disappearance in human liver microsomes, measured from 45 min incubation with human hepatic liver microsomes (1 mg/mL at 37 °C).<sup>23</sup>

substituting the piperazine N4 atom of **1** resulted in incremental Ca<sub>v</sub>3.2 inhibition gains, as detailed in Table 1.

Having succeeded in improving Ca<sub>v</sub>3.2 potency to a level comparable with Mibefradil (Table 1), we set out to systematically modify the adamantane ring of **4** (Scheme 2) to verify the effect on Ca<sub>v</sub>3.2 potency and metabolic stability, as metabolite identification analysis indicated it as the main site of oxidative metabolism. The results from such exploration are summarized in Table 2.

The initial attempts to replace the adamantyl group by known, less bulky and lipophilic surrogates,<sup>14–17</sup> were met with limited success (**5–8**, Table 2). These initial results also clearly indicated that introduction of polarity in that region, while beneficial to metabolic stability, was deleterious to Ca<sub>v</sub>3.2 potency, as exemplified by the

**Table 3**Ca<sub>v</sub>3.2 potency, metabolic stability, hERG and CYP450 2D6 inhibition for compounds in the 'core variation' set

						
Compound	R1	CORE	Ca <sub>v</sub> 3.2 IC <sub>50</sub> <sup>a</sup> (μM)	hERG IC <sub>50</sub> <sup>b</sup> (μM)	HLM Cl <sub>int</sub> <sup>c</sup> (μL/min/mg)	CYP450 2D6 <sup>d</sup> (μM)
<b>4</b>	1-Adamantyl		0.8	32	48	>20
<b>13</b>	3,5-Dichlorophenyl		0.9	1.7	<5	1
<b>14</b>	1-Adamantyl		0.5	15	59	19
<b>15</b>	3,5-Dichlorophenyl		0.3	1.6	13	0.8
<b>16</b>	1-adamantyl		0.8	15	38	10
<b>17</b>	3,5-Dichlorophenyl		0.2	1.2	<5	0.5
<b>18</b>	1-Adamantyl		0.9	26	85	9
<b>19</b>	1-Adamantyl		1.5	—	210	13

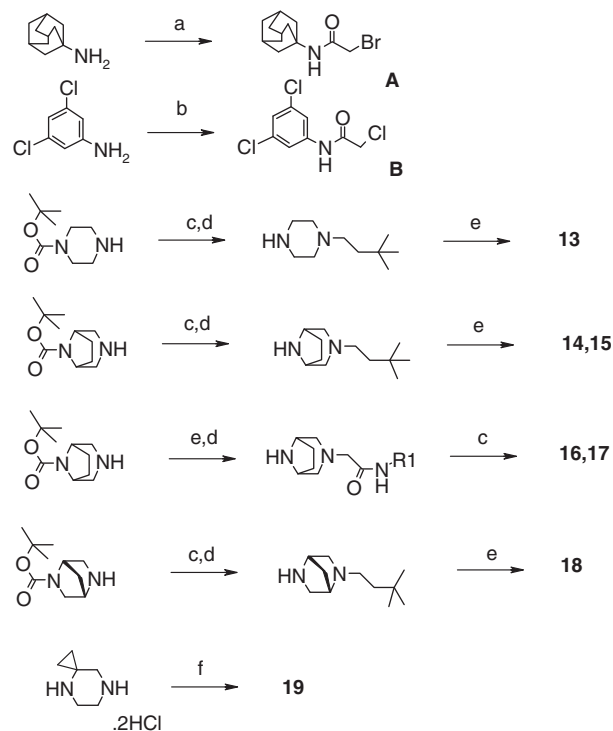
<sup>a</sup> Results are mean of at least two experiments. Experimental errors within 20% of value.<sup>22</sup><sup>b</sup> Patch clamp assay using IONWORKS™ technology in hERG-expressing CHO cells.<sup>c</sup> Rate of disappearance in human liver microsomes, measured from 45 min incubation with human hepatic liver microsomes (1 mg/mL at 37 °C).<sup>23</sup><sup>d</sup> Inhibition of metabolic degradation of MAMC (7-methoxy-4-(aminomethyl)-coumarine) by human recombinant cytochrome P450 2D6 at 37 °C—The percent inhibition is determined at five different concentrations and reported as IC<sub>50</sub>.

matched pairs **4–5** and **6–7** (Table 2). The difficulty in maintaining potency and improving metabolic stability was subsequently confirmed by attempting a more systematic simplification of the adamantyl ring with 1,4-dimethylpentyl (**8**), 2-norbornyl (**9**) and cyclohexyl (**10**) moieties. Substitution on the 4 position of cyclohexane had again the opposite effect on the potency-metabolic stability equation (cf. **11** and **12**, Table 2). Aromatic replacement (**13**) of the adamantyl ring proved successful in combining metabolic stability (HLM Cl<sub>int</sub>: <5 μL/min/mg) with Ca<sub>v</sub>3.2 potency (IC<sub>50</sub>: 0.9 μM).

We then turned our attention to the central core structure and explored substituted piperazine rings in an effort to reduce metabolism originating from N-dealkylation mechanisms, as shown in Table 3. Compounds **14–19** were prepared using standard methods as described in Scheme 3.

Overall, crowding of each of the piperazine nitrogen atoms did not significantly decrease oxidative metabolism of the compounds in the 1-adamantyl subseries, as exemplified by **14**, **16**, and **18** in Table 3. As previously discussed, the 3,5-dichlorophenyl moiety offered a substantial advantage in terms of metabolic stability over the 1-adamantyl ring, while displaying a tendency towards increased Ca<sub>v</sub>3.2 potency (cf. **13** and **4**, Table 3). However, it also yielded a consistent worsening of hERG and CYP450 2D6 inhibition compared to the 1-adamantyl, as exemplified by the matched pairs **4–13**, **14–15** and **16–17** in Table 3. These findings are in agreement with earlier reports on the liabilities associated with aromaticity in drug-like molecules.<sup>18,19</sup>

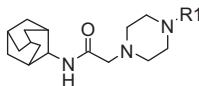
The original adamantyl-containing Ca<sub>v</sub>3.2 inhibitor **4** offered the best combination of Ca<sub>v</sub>3.2 potency, selectivity over the hERG ion channel and CYP450 enzymes, but displayed suboptimal metabolic stability. Having failed to improve on the overall profile of the ligands with chemical modifications of the adamantane and piperazine rings, we focused on the neoheptyl side chain to reduce the degree of oxidative metabolism. Compounds **20–29** were designed to reduce the lipophilic character of the ligands and thus improve metabolic stability, as summarized in Table 4.



**Scheme 3.** Synthesis of the 'core variation' set. Reagents and conditions: (a) 2-bromoacetyl bromide, Na<sub>2</sub>CO<sub>3</sub>, DCM, –65 to 20 °C, 16 h, 77%; (b) 2-chloroacetyl chloride, DIEA, DCM 20 °C, 16 h, 93%; (c) (i) 3,3-dimethylbutyraldehyde, NaBH(OAc)<sub>3</sub>, MeOH, 20 °C, 16 h, (ii) TFA, DCM, 20 °C, 2–16 h, 76–95% over two steps; (d) (i) **A** or **B**, K<sub>2</sub>CO<sub>3</sub>, acetonitrile 110 °C, μw, 10 min or DIEA, DCM, 20 °C, 16 h or *N,N*-(diisopropyl)aminomethylpolystyrene, DCM, 20 °C, 16 h, (ii) TFA, DCM, 20 °C, 2–16 h, 40–90% over two steps; (e) 3,3-dimethylbutyraldehyde, NaBH(OAc)<sub>3</sub>, MeOH, 50 °C, 16 h, 5–20%; (f) **A** or **B**, K<sub>2</sub>CO<sub>3</sub>, acetonitrile 110 °C, μw, 10 min, 25–90%; (g) (i) **A**, DIEA, DCM, 20 °C, 16 h, (ii) 3,3-dimethylbutyraldehyde, NaBH(OAc)<sub>3</sub>, MeOH, 20 °C, 16 h, <5% over two steps.

**Table 4**

Ca<sub>v</sub>3.2 potency, metabolic stability and hERG inhibition for compounds in the 'neoheptyl variation' set

				
Compound	R1	Ca <sub>v</sub> 3.2 IC <sub>50</sub> <sup>a</sup> (μM)	hERG IC <sub>50</sub> <sup>b</sup> (μM)	HLM Cl <sub>int</sub> <sup>c</sup> (μL/min/mg)
<b>4</b>		0.85	32	48
<b>20</b>		3.6	14	94
<b>21</b>		5.0	ND <sup>d</sup>	ND <sup>d</sup>
<b>22</b>		30	ND <sup>d</sup>	<5
<b>23</b>		12	ND <sup>d</sup>	<5
<b>24</b>		9	30	30
<b>25</b>		2	20	<5
<b>26</b>		1.7	>33	72
<b>27</b>		1.9	33	21
<b>28</b>		5.8	33	69
<b>29</b>		0.9	33	18

<sup>a</sup> Results are mean of at least two experiments. Experimental errors within 20% of value.<sup>22</sup>

<sup>b</sup> Patch clamp assay using IONWORKS™ technology in hERG-expressing CHO cells.

<sup>c</sup> Rate of disappearance in human liver microsomes, measured from 45 min incubation with human hepatic liver microsomes (1 mg/mL at 37 °C).<sup>23</sup>

Incorporation of heteroaryl groups in the side chain (**20** and **21**) had a negative effect on Ca<sub>v</sub>3.2 potency, and the most potent derivative (**20**) still displayed very high intrinsic clearance, as shown in Table 4. On the other hand, compounds containing saturated heterocycles (**22–25**) showed increased metabolic stability, whereas the impact on Ca<sub>v</sub>3.2 affinity was variable. Replacement of a morpholine group with a tetrahydropyran (**23** and **25**, respectively) proved successful in combining acceptable potency (Ca<sub>v</sub>3.2 IC<sub>50</sub>: 2 μM) and metabolic stability (HLM Cl<sub>int</sub>: <5 μL/min/mg). Heteroaliphatic side chains displayed improved Ca<sub>v</sub>3.2 potency and selectivity over the hERG channel but, unfortunately, moderate to high intrinsic clearance (**26–29**, Table 4). The two enantiomers of compound **29** were separated by chiral HPLC but displayed similar potency and clearance values (data not shown).

Compound **25** emerged as an adequate Ca<sub>v</sub>3.2 inhibitor for further profiling, as outlined in Table 5. Compared to Mibefradil, it showed enhanced selectivity over a range of ion channels of cardiovascular importance (notably the L-type calcium channel—Ca<sub>v</sub>1.2) and CYP450 enzymes, and a comparable pharmacokinetic

**Table 5**

In vitro/vivo comparison of **25** and Mibefradil

	<b>25</b>	Mibefradil
Ca <sub>v</sub> 3.2 IC <sub>50</sub> <sup>a</sup> (μM)	2	1
Ca <sub>v</sub> 1.2 IC <sub>50</sub> <sup>b</sup> (μM)	>31.6	3
hERG IC <sub>50</sub> <sup>c</sup> (μM)	20	3.3
Na <sub>v</sub> 1.5, I <sub>Ks</sub> , K <sub>v</sub> 4.3 IC <sub>50</sub> <sup>c</sup> (μM)	>33	3.8, 22, 24
'Worst' CYP450 IC <sub>50</sub> <sup>d</sup> (μM)	>20	0.06 (3A4, 2D6)
HLM Cl <sub>int</sub> <sup>e</sup> (μL/min/mg)	<8	57
Human PPB F <sub>u</sub> <sup>f</sup> (%)	53	0.5
Rat PPB F <sub>u</sub> <sup>f</sup> (%)	39	2.5
Rat dose iv/po <sup>g</sup> (μmol/kg)	5/2	1/3
Rat CL <sup>g</sup> (mL/min/kg)	42.5	59.3
Rat F <sup>g</sup> (%)	59	50

<sup>a</sup> Results are mean of at least four experiments. Experimental errors within 20% of value.<sup>22</sup>

<sup>b</sup> Patch clamp assay using IONWORKS™ technology in CHO cells expressing CACNA1C, CACNB2 and CACNA2D1 (ChanTest, Cleveland, OH).<sup>24</sup>

<sup>c</sup> Patch clamp assay using IONWORKS™ technology in CHO cells expressing the relevant human ion channel.

<sup>d</sup> Inhibition of metabolic degradation of the corresponding substrate by human recombinant cytochrome P450s (3A4, 2C9, 2C19, 2D6, 1A2, 2C8) at 37 °C—The percent inhibition is determined at five different concentrations and reported as IC<sub>50</sub>.

<sup>e</sup> Rate of disappearance in human liver microsomes, measured from 45 min incubation with human hepatic liver microsomes (1 mg/mL at 37 °C).<sup>23</sup>

<sup>f</sup> % Fraction unbound in plasma measured by equilibrium dialysis (18 h at 37 °C).

<sup>g</sup> Pharmacokinetic parameters calculated from noncompartmental analysis concentrations in fasted Sprague–Dawley female rats (iv n = 12; po n = 2).

profile in rats (Table 5). Additionally, a selectivity screening including 98 biological targets<sup>20</sup> did not reveal any significant hits (>50% binding) other than the σ<sub>1</sub> receptor, when **25** was tested at a concentration of 10 μM.

As Ca<sub>v</sub>3.2 calcium channels are highly expressed in the sinoatrial node and are known to contribute to cardiac pacemaking in the adult heart,<sup>8</sup> in vivo Ca<sub>v</sub>3.2 inhibition would result in heart rate (HR) reduction. This therefore provides a practical surrogate biomarker to evaluate target engagement in vivo, and to derive pharmacokinetic–pharmacodynamic (PK–PD) relationships for Ca<sub>v</sub>3.2 inhibitors. We thus hypothesized that free plasma concentrations of a Ca<sub>v</sub>3.2 inhibitor equivalent to the IC<sub>50</sub> measured in vitro (assuming no considerable species differences wrt potency) would be sufficient to elicit a significant HR reduction in vivo. Accordingly, based on in vitro Ca<sub>v</sub>3.2 potency (IC<sub>50</sub>: 2 μM), rat plasma protein binding (F<sub>u</sub>: 39%) and the preliminary rat PK profile (Table 5), a 50 μmol/kg dose of **25** was infused to rats,<sup>21</sup> as summarized in Figure 2.

Thirty minutes infusion of **25** significantly reduced HR compared to vehicle (*p* < 0.05). After termination of compound infusion, HR tended to recover toward baseline (Fig. 2). According to the expected physiology of the rat system employed, the HR reduction led to a 8–26% blood pressure reduction during compound infusion. The HR reduction caused by **25** occurred in a concentration-dependent fashion with an effective unbound concentration causing 10% HR reduction estimated to be 1.9 μmol/L (Fig. 2). While there might be differences between in vitro and in vivo potencies as well as potency differences across species, the free plasma concentrations of **25** did not exceed 4 μmol/L in this experiment, thus minimizing the risk for off-target-mediated effects (cf. Table 5).

In summary, starting from a HTS-based fragment hit, a novel series of *N*-(1-adamantyl)-2-(4-alkylpiperazin-1-yl)acetamide-containing Ca<sub>v</sub>3.2 inhibitors was designed by systematic chemical variation of its structural elements. Simultaneous optimization of Ca<sub>v</sub>3.2 potency, ion channel and CYP450 selectivity, as well as metabolic stability identified *N*-(1-adamantyl)-2-[4-(2-tetrahydropyran-4-ylethyl)piperazin-1-yl]acetamide (**25**) as an in vivo efficacious Ca<sub>v</sub>3.2 inhibitor. Further medicinal chemistry optimization

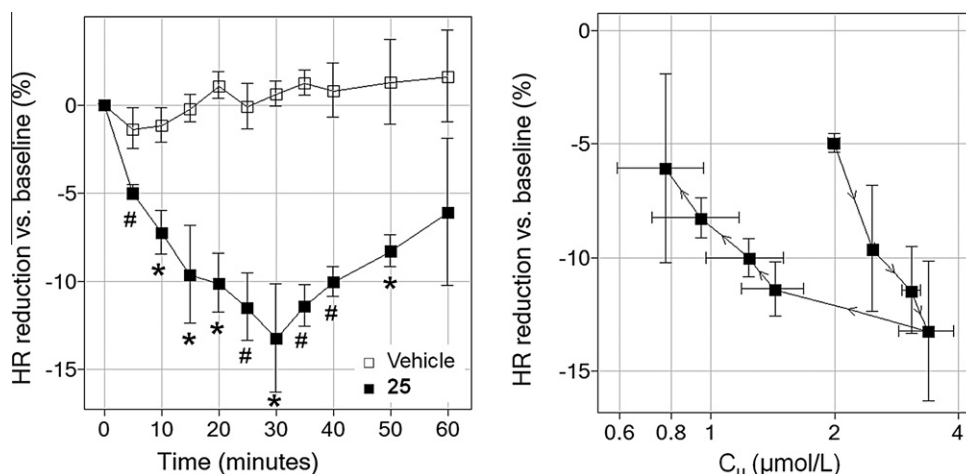


**Figure 2.** HR effect in anaesthetized rats, following infusion of 50  $\mu\text{mol/kg}$  of **25** (solid squares). (left) Comparison to vehicle (squares): (\*)  $p < 0.05$  (#)  $p < 0.02$ ; (right) PK–PD relationship: arrows denote time course of infusion. Error bars indicate standard deviation of measurements.

to validate the hypothesis of a  $\text{Ca}_v3.2$ -mediated cardioprotective effect in atrial fibrillation will be published in due course.

## References and notes

- Ertel, E. A.; Campbell, K. P.; Harpold, M. M.; Hofmann, F.; Mori, Y.; Perez-Reyes, E.; Schwartz, A.; Snutch, T. P.; Tanabe, T.; Birnbaumer, L.; Tsien, R. W.; Catterall, W. A. *Neuron* **2000**, 25, 533.
- Talley, E. M.; Cribbs, L. L.; Lee, J. H.; Daud, A.; Perez-Reyes, E.; Bayliss, D. A. *J. Neurosci.* **1999**, 19, 1895.
- Van der Vring, J. A.; Cleophas, T. J.; Van der Wall, E. E.; Niemeyer, M. G. *Am. J. Ther.* **1999**, 6, 229.
- Sen, L.; Smith, T. W. *Circ. Res.* **1999**, 75, 149.
- Fareh, S.; Benardeau, A.; Thibault, B.; Nattel, S. *Circulation* **1999**, 100, 2191.
- Fareh, S.; Benardeau, A.; Nattel, S. *Cardiovasc. Res.* **2001**, 49, 762.
- Satoh, H. *Gen. Pharmacol.* **1995**, 26, 581.
- Ono, K.; Iijima, T. *J. Mol. Cell. Cardiol.* **2010**, 48, 65.
- Kuga, T.; Sadoshima, J.; Tomoike, H. *Circ. Res.* **1990**, 67, 469.
- Chen, C.-C.; Lamping, K. G.; Nuno, D. W.; Barresi, R.; Prouty, S. J.; Lavoie, J. L.; Cribbs, L. L.; England, S. K.; Sigmund, C. D.; Weiss, R. M.; Williamson, R. A.; Hill, J. A.; Campbell, K. P. *Science* **2003**, 302, 1416.
- Giordanetto, F.; Knerr, L.; Wällberg, A. *Exp. Op. Ther. Pat.* **2011**, 21, 85.
- Vassort, G.; Talavera, K.; Alvarez, J. L. *Cell Calcium* **2006**, 40, 205.
- Yang, Z. Q.; Barrow, J. C.; Shipe, W. D.; Schlegel, K. A.; Shu, Y.; Yang, F. V.; Lindsley, C. W.; Rittle, K. E.; Bock, M. G.; Hartman, G. D.; Uebele, V. N.; Nuss, C. E.; Fox, S. V.; Kraus, R. L.; Doran, S. M.; Connolly, T. M.; Tang, C.; Ballard, J. E.; Kuo, Y.; Adarayan, E. D.; Prueksaritanont, T.; Zrada, M. M.; Marino, M. J.; Graufelds, V. K.; DiLella, A. G.; Reynolds, I. J.; Vargas, H. M.; Bunting, P. B.; Woltmann, R. F.; Magee, M. M.; Koblan, K. S.; Renger, J. J. *Med. Chem.* **2008**, 51, 6471.
- Villhauer, E. B.; Brinkman, J. A.; Naderi, G. B.; Burkey, B. F.; Dunning, B. E.; Prasad, K.; Mangold, B. L.; Russell, M. E.; Hughes, T. E. *J. Med. Chem.* **2003**, 46, 2774.
- Guile, S. D.; Alcaraz, L.; Birkinshaw, T. N.; Bowers, K. C.; Ebdon, M. R.; Furbur, M.; Stocks, M. J. *J. Med. Chem.* **2009**, 52, 3123.
- Sorensen, B.; Rohde, J.; Wang, J.; Fung, S.; Monzon, K.; Chiou, W.; Pan, L.; Deng, X.; Stolarik, D.; Frevert, E. U.; Jacobson, P.; Linka, J. T. *Bioorg. Med. Chem. Lett.* **2006**, 16, 5958.
- Olson, S.; Aster, S. D.; Brown, K.; Carbin, L.; Graham, D. W.; Hermanowski-Vosatka, A.; LeGrand, C. B.; Mundt, S. S.; Robbins, M. A.; Schaeffer, J. M.; Slossberg, L. H.; Szymonifka, M. J.; Thieringer, R.; Wright, S. D.; Balkovec, J. M. *Bioorg. Med. Chem. Lett.* **2005**, 15, 4359.
- Lovering, F.; Bikker, J.; Humblet, C. *J. Med. Chem.* **2009**, 52, 6752.
- Ritchie, T. J.; Macdonald, S. J. *Drug Discovery Today* **2009**, 14, 1011.
- Ricerca Biosciences, LLC 7528 Auburn Road Concord, OH 44077 US A.
- Adult Sprague–Dawley rats (BW 300–350 g,  $N = 3$ ) were anaesthetized with pentobarbital sodium and placed on a heating pad to keep the body temperature at 38 °C throughout the experiment. The animals were ventilated with a Ugo ventilator at a frequency of 60 cycles/min and 2 mL/breath. A PE50 catheter was put into the jugular vein for substance infusion and another PE50 catheter into a carotid artery for blood pressure measurements and blood sampling. To achieve autonomic blockade, both left and right vagal nerves were cut and Metoprolol (5 mg/kg iv) was given 20 min prior to start of substance infusion. Test compound or vehicle (0.1 mL/kg/min) was infused over 31 min followed by 75 min of washout. Blood was taken, for analysis of plasma level of test compound, before start of infusion and at 5, 15, 25, and 30 min of infusion as well as 5, 10, 30, 50, and 75 min of washout. Lead II ECG was registered and heart rate was analyzed using PharmLab (AstraZeneca) software.
- A stable cell line was constructed by transfecting T-Rex 293 cells (Life Technology Corp., Carlsbad, CA) with a pcDNA4TO vector encoding human CACNA1H. Patch-clamp measurements were performed in the standard whole cell configuration using a QPatchHTX instrument (Sophion Bioscience A/S, Ballerup, Denmark). The extracellular solution contained (mM): NaCl 145, KCl 4,  $\text{CaCl}_2$  2,  $\text{MgCl}_2$  1, HEPES 10, glucose 10 (pH 7.4) and the intracellular (mM): KCl 120,  $\text{MgCl}_2$  1.75,  $\text{CaCl}_2$  5.374, EGTA 10, HEPES 10,  $\text{Na}_2\text{ATP}$  4 (pH 7.2). All experiments were performed at room temperature. The cells were depolarized from a holding potential ( $V_{\text{hold}}$ ) of  $-100$  or  $-80$  to  $-20$  mV. Compound **25** blocked the t-type current in a concentration dependent manner with an  $\text{IC}_{50}$  of  $2.0 \pm 0.4 \mu\text{M}$  ( $n = 4$ ) at  $V_{\text{hold}} = -100$  mV and  $3.7 \pm 0.6 \mu\text{M}$  ( $n = 5$ ) at  $-80$  mV ( $p < 0.05$  vs  $V_{\text{hold}} = -100$  mV). The compound had no effect on the current voltage relationship, steady-state activation ( $V_{1/2} = 45 \pm 3$  vs  $46 \pm 1$  mV,  $n = 5$ ,  $p = \text{n.s.}$ ), steady-state inactivation ( $V_{1/2} = 60 \pm 3$  vs  $59 \pm 2$ ,  $n = 5$ ,  $p = \text{n.s.}$ ) or recovery after inactivation ( $\tau = 299 \pm 27$  vs  $303 \pm 26$  ms, respectively,  $n.s.$ ).
- Test compounds (6  $\mu\text{L}$  of 50  $\mu\text{M}$  DMSO/MeCN) are incubated with liver microsomes\* (1 mg/mL in 0.1 M phosphate buffer pH 7.4) and NADPH (0.5 mM in phosphate buffer pH 7.4) in a 96-well plate at 37 °C. An aliquot of the incubation mixture is taken after 0, 5, 15, and 45 min and the reaction is stopped with cold acetonitrile containing volume marker (1 mM 5,5-diethyl-1,3-diphenyl-2-iminobarbituric acid). The samples are centrifuged at 4000 rpm and supernatant is transferred and diluted with water in 96 well plates. The intrinsic metabolic capacity, measured as intrinsic clearance ( $\text{CL}_{\text{int}}$ ) gives an indication of the contribution of hepatic oxidative metabolism to the overall clearance of the test compound. Calculation of  $\text{CL}_{\text{int}}$  is based on the substrate disappearance rate. The chromatographic peaks are integrated and a linear plot of  $\ln$  areas vs. time is created. The slope is calculated for each data set.  $T_{1/2}$  and  $\text{CL}_{\text{int}}$  are calculated according to the following equations:  

$$T_{1/2} = \ln 2 / -\text{slope}$$

$$\text{CL}_{\text{int}} = \ln 2 \cdot 1000 / T_{1/2} \cdot [\text{protein}]$$
- Dilbaghi, S.; Abi-Gerges, N.; Morton, M. J.; Bridgland-Taylor, M. H.; Pollard, C. E.; Valentin, J.-P. *J. Pharmacol. Toxicol. Methods* **2010**, 62, e1.